Proceedings of the ASME 2015 Gas Turbine India Conference
GTINDIA2015
December 2-3, 2015, Hyderabad, India

GTINDIA2015-1202

UNIVERSAL MODELING METHOD – THE INSTRUMENT FOR CENTRIFUGAL COMPRESSOR GAS DYNAMIC DESIGN

Y. Galerkin, A. Rekstin, K. Soldatova, A. Drozdov
R&D Laboratory "Gas dynamics of turbo machines"
Joint Institute of Science and Technology
Peter the Great St.Petersburg Polytechnic University
195251, St.Petersburg, Polytechnicheskaya, 29
Russia
e-mail: galerkin@pef.spbstu.ru

ABSTRACT

Similarity theory principles are widely applied in gas dynamic design. But completely new solutions must be realized on a base of engineering approaches to predict performances. The heart of the Universal modeling engineering method is the physical model that is based on flow visualization and measurements inside rotating impellers. The math model is a sum of algebraic equations for calculation of head losses. Normalized velocity gradients along and normal to blade surfaces are arguments. Empirical coefficients values are established in a course of the identification – calculated performances are compared with the measured ones for several dozens of model stages tests with wide range of design parameters. The 4th version of the TU SPb modeling method (the set of the several computer programs) was applied in design practice in 1993 – 2010. Some Russian and foreign manufacturers realized several dozens of designed compressors with power up to 25 MW. The level of design point parameters prediction was so satisfactory that the manufacturers do not prove designs by model tests anymore. The whole performance prediction was not so good. The other difficulty – to predict design point efficiency with accuracy about 0,5% the very careful choice of empirical coefficients is necessary. The difficulties have been overcome in the new 5th and 6th versions. Most effective multistage compressors plant test performances were modeled successfully by 5th version program with the single set of empirical coefficients. Calculated performances and geometry of several dozens of stages of these compressors can be are applied in designs as usual model stages. The current designs are executed by the 5th and 6th version computer programs. The single stage 32 MW pipe line compressor was recently designed for the Ukrainian partner who offered high-RPM drive and favorable single-stage scheme. The test of the model at the 1:2 scale validated project parameters. Design pressure ratio and efficiency curves have matched completely. The predicted maximum efficiency 90% was proven.

NOMENCLATURE

c_2	absolute velocity at an impeller exit;
c_w	friction force coefficient; Critical streamlines change directions near blade edges.
$\Delta\bar{c}_{u1}$	inlet critical streamline pre-rotation due to blade load related to u_2;
$\Delta\bar{c}_{u2}$	outlet critical streamline post-rotation due to blade load related to u_2;
h_w	loss of head;
k	isentropic coefficient;
K_μ	empirical coefficient (viscosity influence on a loading factor);
M_u	blade Mach number;
$\bar{m}$	mass flow rate;
N_i	compressor shaft power;
p	pressure;

R gas constant;
Re_u impeller diameter Reynolds number;
Ro' non-dimensional normal velocity gradient;
T temperature;
u_2 blade velocity;
w_1 relative velocity at an impeller inlet;
$w_{\sec}$ velocity of a secondary flow;
X_i empirical coefficient in math model;
z number of blades;
β_{fr} disc friction coefficient;
β_{leac} shroud disc labyrinth seal leakage coefficient;
β_{bl} blade angle to tangential direction;
α_2 flow angle at an impeller exit;
$\lambda_{w\max}$ maximum velocity coefficient on a blade surface;
π pressure ratio;
τ blockage effects coefficient in cascade;
φ_2 flow rate coefficient at an impeller exit;
ψ_p polytrophic head coefficient;
ψ_i work coefficient;
ψ_T loading factor;
$\psi_{T\,des}$ design loading parameter;
ω angular velocity;
$\Delta\eta$ loss of efficiency;
$\Delta\eta_{imp}$ loss of efficiency in an impeller;
η - polytrophic efficiency;
Φ flow rate coefficient;
Φ_{des} design flow rate coefficient;
ζ_{imp} loss coefficient of an impeller;
$\zeta_{mix\,s}$ coefficient of mixing losses;
ζ_{fr} coefficient of friction losses.

SUBSCRIPTS

1 impeller blade row inlet;
2 impeller outlet;
bl blade;
des design;
h hub;
imp impeller;
inc incidence;
max maximum;
mix mixing;
s shroud.

INTRODUCTION. CENTRIFUGAL COMPRESSOR ROLE AND GAS DYNAMIC PROBLEMS

This kind of compressors is applied in all basic industries and their installed power is great. In Russian pipeline industry only operate 4 484 compressor units with total power 51 000 000 kW (December 2014). Additional 540 units with total power 11 000 000 kW must be put in operation in visible future. Comparable amount of compressors operate in all basic industries. Industrial compressors life time is 3 – 4 decades. Many compressors are old. Development and renovate processes in chemistry, metallurgy, etc. are increasing demand for new compressors. Energy saving prevails when industrial compressor is designed. The first step is gas dynamic design.

There are many effective compressors now that are the base for new designs by application of the similarity theory. Nevertheless the world engineering companies offer their service in absolutely new gas dynamic design and find clients [1, 2]. The team of the authors designs 2-4 new centrifugal compressors annually [3].

The challenge of a new design consists of the next:

- given pressure ratio must be guaranteed at given mass flow rate,
- efficiency must be as high as possible at a design point and in the widest range of flow rate,
- surge limit must be as far as possible from a design flow rate,
- special demands for gas dynamic curves – maximum power must be at a design flow rate for GT driven compressors,
- mechanical limitations must be taken into account.

Recommendations to choose main dimensions of a flow path are presented in books [3, 4, 5, 6, 7], etc. The corresponding designs would be not absurd. But the listed above demands cannot be guaranteed. The performance curves of the new design must be defined and must be compared with a buyer technical specification. The model tests were a solution at pre-computer era. CFD calculations are offered now instead. The authors are not so sure in centrifugal compressor performance curves validity calculated by CFD [8, 9]. The positive experience of CFD calculations of stator elements [8, 9] does not change the situation. The engineering methods of design and quantitative analysis are actual as ever. There is a quotation from the text that belongs to one of leading western specialists [1]: "Some turbo machine engineers believe that the project can be begun with application of methods of computing gas dynamics – nothing can be further from truth. By the one-dimensional analysis it is necessary to find optimum triangles of velocities, inlet blade angles, middle radiuses, height of channels".

The way to calculate compressor performance curves $\pi, \eta, N_i = f\left(\bar{m}\right)$ is simple when non-dimensional stage performance curves $\psi_i, \eta = f\left(\Phi\right)$ are known:

$$\pi = \left(1 + \left(k-1\right)\psi_i M_u^2\right)^{\frac{k}{k-1}\eta} \qquad (1)$$

Where $\Phi = \dfrac{4\bar{m}}{\pi\rho_{0t} D_2^2 u_2}$.

Stage performances are objects of math modeling. The author of [1] prefers application of boundary layer theory methods. Empirical coefficients are defined on a base of experimental performances of a stage flow path elements. Authors of [10] use simple hydraulic analogies, as a diffuser divergence angle, etc. The authors of the presented work continue to develop ideas formulated still in 1970t^{h} and presented in detail in [5]. Math model takes into account flow behavior. Physical model reduces flow behavior to a simplified scheme. Math model calculates loss coefficients of stage elements by algebraic equations with normalized non-viscid core velocity gradients as arguments.

FLOW BEHAVIOR

The physical model takes into account flow behavior that has been studied by measurements and flow visualization. The summarizing of vast experiments is presented in [3]. Two samples of the visualization are presented at Fig.1.

Thin powder inserted in the flow path sticks to surfaces with low shear stresses visualizing separation zones (Fig. 1). The known "jet-wake" phenomenon is detected. The wake is of 3D character. Wake formation takes place at a suction side at positive incidences, and at a design flow rates in most cases too. Flow velocity near a shroud is the biggest and its deceleration leads to earlier jet formation near a shroud. There is the zone of low shear stress in the corner near a hub. This zone is formatted by a secondary flow on a hub surface.

The special water test rig was constructed to study flow stream lines close to surfaces. Flow traces on wet oil paint that were left by water flow are shown at the photo – Fig. 1. Wake starts at a leading edge near a shroud at this flow rate. Jet-wake model is proven by experiments. Meridional velocity in a wake is about 20% of a jet velocity. There is no backward flow from a diffuser to an impeller.

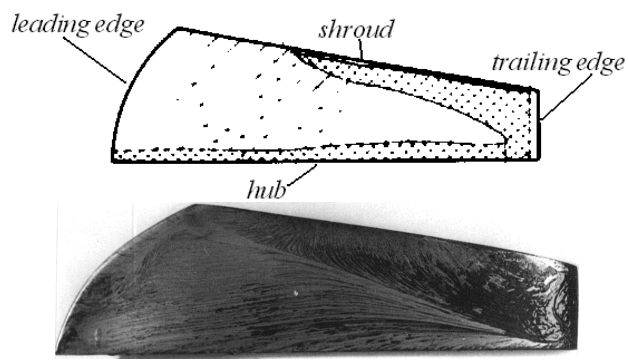

FIGURE 1. SUCTION SIDE OF 2D IMPELLER FLOW VISUALIZATION. LEFT - LOW SHEAR STRESS ZONE AT A DESIGN FLOW RATE (AIR TEST), RIGHT – SURFACE FLOW LINES AT A SURGE LIMIT FLOW RATE (WATER TEST) [5]

The important fact is that there is no flow separation at blades' pressure side at any flow rate. No flow separation was detected at hub and shroud surfaces at any flow rates. The phenomenon was explained by Prof. E. Smirnov (TU SPb). Secondary flow produces the Coriolis acceleration $2\omega \cdot w_{\sec}$ oriented in the same direction as a core flow. The result is thin boundary layers with shear stresses preventing separation.

The single-point pressure transducer with the switch for 33 points was invented and constructed for pressure measurements inside impellers (maximum RPM 18 000). Velocity diagrams at design (Φ_{des} = 0,0852) and off – design flow rates are shown at Fig. 2.

The measured diagrams are based on measured static pressure and calculated total pressure inside an inviscid core. The computer program 3DM-023 for non-viscid quasi – 3D calculations the authors apply in design practice from 1990–th [3]. Axis-symmetrical flow is calculated by quasi-orthogonal method. Blade-to-blade solution on 7 surfaces along blade height is made by integral equation method. Blades are substituted by vortexes. Non-penetration condition is achieved in course of iterations. The advantage of the solution is correct calculation of flow near leading and trailing edges. Kutta-Joukowski condition for trailing edges is applied. The flow character near a leading edge is predicted well. It gives the possibility to design an impeller with non-incidence inlet at a design flow rate. Experiments demonstrate that non-incidence inlet leads to the highest possible efficiency. It is one of conditions to reach highest efficiency. Both diagrams are very alike at a design flow rate. The principal difference is in a part where flow separation starts (very close to a trailing edge in case of the impeller that is shown at Fig. 2). Q3D calculations are applied for 2D and 3D impeller blade shape optimization – non-incidence inlet along a leading edge height, necessary loading factor, mean blade load, control of velocity deceleration along suction side. All this is important to obtain maximum efficiency.

A loading factor is proportional to an area of a velocity diagram. An area of a calculated diagram is close to an area of a measured one. The empirical coefficient correlates their values. Q3D calculations are used as the final step of the load factor definition. It is a technique to guarantee given pressure ratio.

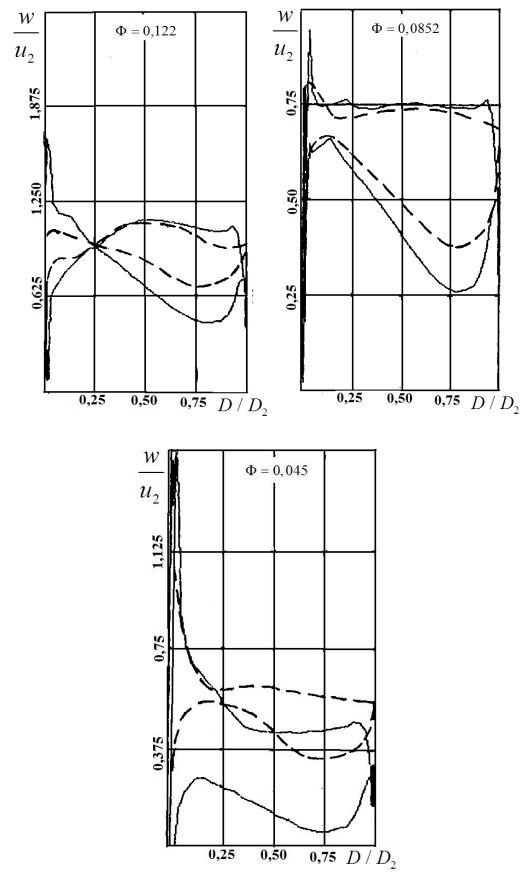

FIGURE 2. VELOCITY DIAGRAMS AT THE 2D IMPELLER BLADE AT THREE FLOW RATES. SOLID LINES – Q3D NON-VISCID CALCULATION, STROKE LINES – MEASURED

HEAD LOSS MODEL

The principles that are presented below were realized in the 4th version of the model and computer programs that were widely applied in R&D practice since mid-1990th [3]. The level of design point parameters prediction was so satisfactory that the manufacturers do not prove new compressors by model tests anymore. The whole performance prediction was not so good. The other difficulty – to predict design point efficiency with accuracy about 0,5% the different sets of empirical coefficients for stages with different design parameters are necessary.

The problems were solved in the 5th version [11, 12, 13] applied to stages with traditional 2D impellers and VLD. The 6th version widens this principle for other types of stages that was forced to add

some further improvements. The general principles of modeling and some special features of new models are presented below.

The principle of loss summarizing is usual in engineering calculation and analysis:

$$\eta = \frac{1 - \sum \Delta\eta}{1 + \beta_{fr} + \beta_{leac}} \tag{2}$$

Here $\Delta\eta$ is loss of efficiency of in of flow path elements: inlet nozzle, impeller, vaneless diffuser, vane diffuser, return channel or exit nozzle (volute, etc.). By tradition work coefficient is presented as a product of mechanical work transmitted to a gas by blades – loading factor ψ_T, by outer disc surfaces β_{fr} and work, provided by blades to a gas flow in a shroud disc labyrinth seal β_{leac}:

$$\psi_i = \psi_T \left(1 + \beta_{fr} + \beta_{leac}\right) \tag{3}$$

If $\bar{c}_{u1} = 0 \quad then \quad \psi_T = \bar{c}_{u2}$.

The disc friction coefficient β_{fr} and labyrinth leakage β_{leac} are calculated by well proven semi-empirical way [14]. In case of an impeller:

$$\Delta\eta_{imp} = \frac{\zeta_{imp}}{2\psi_T} \bar{w}_1^2 \tag{4}$$

The loss coefficient of an impeller blade cascade reflects the fact of absence of mixing losses everywhere but a suction side of blades (different kinetic energy at suction and pressure sides of blades is taken into account too):

$$\zeta_{imp} = \left(\zeta_{fr\,s} + \zeta_{mix\,s}\right)\left(\frac{\bar{w}_{1s}}{\bar{w}_1}\right)^2 + \zeta_{fr\,s}\left(\frac{\bar{w}_{1p}}{\bar{w}_1}\right)^2 + \zeta_{fr\,hub} + \zeta_{fr\,shr} \tag{5}$$

The object of friction loss modeling is the friction drag force coefficient. There are equations of the Russian aerodynamic – classic [15] for thin plate coefficient – rough and hydraulically smooth surfaces (turbulent flow without velocity gradients). Empirical coefficients $X(i)$ are inserted in math model:

$$c_{f\,smooth} = X(i)\frac{0{,}0307}{\mathrm{Re}_w^{1/7}} \tag{6}$$

$$c_{f\,rough} = \frac{X(i)}{1{,}89 + 1{,}62\lg\left(1/k_{rg}\right)^{2{,}5}} \tag{7}$$

The 4th version used the Eq. (6), treating flow path surfaces as hydraulically smooth. The new 5th and 6th versions take surface roughness into account by Eq. (7).

Velocity gradients in a compressor flow path influence friction losses. Math model representation is:

$$c_w = c_f\left(1 + X(i)\left|Ro'\right|\right)^{X(i)} + X(i)\left(1 - \dot{w}\right)^{X(i)} \tag{8}$$

There parameter Ro' is a non-dimensional normal velocity gradient. For impeller blades it is:

$$Ro' = 4 - \frac{\bar{w}_{mean}}{\bar{R}_{bl\,mean}}. \tag{9}$$

The empirical coefficients $X(i)$ take into account flow path difference from the simplified model – thin plate. Velocity gradients influence boundary layers parameters, shear stress in particular.

The interconnection of ζ_{fr} and c_w establishes the equation of a power loss calculated on a base of these parameters:

$$\zeta_{fr\,bl} = 0{,}5\frac{c_{wbl} z \varepsilon_{mean} \bar{S}_{bl}}{\Phi_0}\left(\left(\frac{\bar{w}_{s\,mean}}{\bar{w}_1''}\right)^2 \bar{w}_{s\,mean} + \left(\frac{\bar{w}_{p\,mean}}{\bar{w}_1''}\right)^2 \bar{w}_{p\,mean}\right) \tag{10}$$

- blade surfaces,

$$\zeta_{fr\,o} = 0{,}125 c_{wo}\frac{\varepsilon_{mean}}{\Phi_0}\bar{S}_o\left(1 + \dot{w}\right)^3 \cdot \bar{w}_1'' \tag{11}$$

- hub and shroud surfaces.

Mixing loss model is based on equation of sudden expansion $h_{mix} = 0{,}5\left(w_1 - w_2\right)^2$. The "jet-wake" model supposition is that flow is leaving an impeller in a jet, while flow meridian component is zero in a wake. Mixing losses are proportional to difference of a jet meridian component and a meridian component of fully uniform flow after mixing. The empirical coefficient takes into account the real character of flow:

$$\zeta_{mix\,imp} = X(i)\frac{\left(\varphi_{2\,jet} - \varphi_2'\right)^2}{\bar{w}_1''^2} \tag{12}$$

Where $\varphi_2' = \bar{c}_{m2}'$, $\varphi_{2\,jet} = \bar{c}_{m2\,jet}'$.

Calculations by 4th version indicate that Eq. (11) underestimates mixing losses in impellers with high loading factor. In 5th and 6th versions the empirical coefficient is presented as function of this parameter:

$$X_{20} = X(i)\left(1 + X(i)\psi_T^{X(i)} + X(i)\left(1 - \dot{w}\right)^{X(i)}\right). \tag{13}$$

Flow deceleration to a separation point (suction side) was presented as function of Ro' in the 4th version (Eq. 14). More representatives are a loading factor (Eq. 14a):

$$\dot{w}_s = X(i)\left(1 + X(i)Ro'^{X(i)}\right) \tag{14}$$

$$\dot{w}_s = X(i)\left(1 + X(i)\psi_T^{X(i)}\right) \tag{14a}$$

Experiments have demonstrated that the velocity coefficient influence on losses depends on its maximum value on a profile near the leading edge at a suction side:

$$K_M = 1 + X(i)\lambda_{w_{s1}}^{X(i)}, \tag{15}$$

velocity coefficient is defined by equation $\lambda_{w_{s1}} = w_{s1} / \sqrt{\frac{2k}{k+1} R T_{0tot}}$.

Reynolds number and roughness influence is taken into account by eq. (6), (7).

The problem above is treated in 2D mode. Real 3D flow character is modeled by the proper coefficients. In case of a 3D impeller:

$$K_{3D} = 1 + X(i)\left(\frac{\bar{D}_0 - \bar{D}_h}{\bar{D}_h}\right)^{X(i)} \qquad (16)$$

The loss coefficient by Eq. (5) corresponds to non-incidence inlet flow rate. Flow velocity vector $\vec{w}$ is changing in an impeller throat (vector $\vec{w}_1''$ in a throat) when flow direction does not correspond to an inlet blade angle. The model for incidence losses is based on the principle of sudden expansion: $h_{winc} = 0,5\left(\vec{w}_1'' - \vec{w}_1\right)$. The Eq. (17) realizes these principle meaning inlet velocity triangles components:

$$\Delta\eta_{inc} = X(i)(1 + X(i)(\lambda_u \bar{w}_1'')^{X(i)}) \frac{\Delta\bar{w}_{1inc}^2}{2\psi_T} \qquad (17)$$

Inlet flow becomes non-uniform in circumferential direction because of blades' load. Critical streamline obtains a negative circumferential component $\Delta c_{u1} < 0$. Streamlines in mid-span obtain $\Delta c_{u1} > 0$. The non-dimensional critical streamline circumferential component $\Delta\bar{c}_{u1}$ is taken into account in a process of incidence loss calculation. It is shown in a scheme presented in Fig. 3.

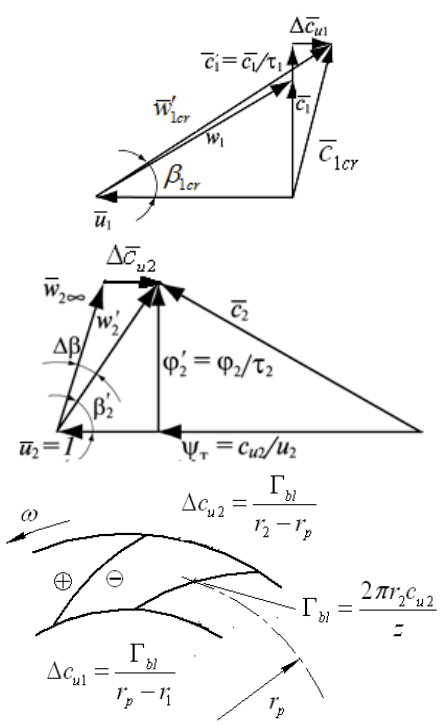

FIGURE 3. SCHEME FOR CRITICAL STREAMLINES DIRECTION DEFINITION

Pressures are different at blade surfaces $p_s < p_p$ (plus – minus symbols at Fig. 3). Critical streamlines change directions near blade edges. Velocity triangle components $\Delta\bar{c}_{u1}$ and $\Delta\bar{c}_{u2}$ are results of a blade load. The proposed model substitutes a blade by a swirl with the same circulation as a blade. A swirl creates $\Delta\bar{c}_{u1}$ and $\Delta\bar{c}_{u2}$. Non incidence condition for a design blow rate is:

$$\beta_{1des} = \beta_{1bl} = arctg \frac{\varphi_1'}{\bar{D}_1 - \Delta\bar{c}_{u1}}, \quad \left(\Delta\bar{c}_{u1} < 0\right) \qquad (18)$$

The models for stator part elements are based in the same principles and were revised in the new versions of the model.

One of improvements realized in 5th version and used in 6th version is the more accurate velocity diagram schematization. Velocities near edges at both blade surfaces are necessary to know. Maximum velocity is necessary to calculate velocity coefficient $\lambda_{w\max}$ that influences head losses. Solid thick lines in Fig 4 demonstrate simplified schematization of velocity diagrams. Inlet and outlet velocities are known from 1D calculation. Blade load Δw depends on a loading factor and number of blades. Velocities at suction and pressure sides are $w_{suct} = w + 0,5\Delta w$, $w_{press} = w - 0,5\Delta w$. Numerical Q3D analysis of about 100 impellers of modern design has given information about velocity diagrams that are close to real diagrams. The results were approximate by algebraic equations. The effect demonstrates Fig. 4 (thin lines).

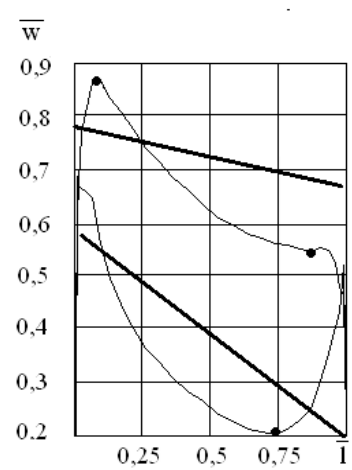

FIGURE 4. NON-VISCID VELOCITY OF IMPELLER BLADES DIAGRAM AND ITS SCHEMATIZATION. SOLID LINES – 'TRAPETHOID" REPRESENTATION IN THE 4TH VERSION, DOTS – CALCULATION BY EQUATIONS THAT APPROXIMATES NUMERICAL EXPERIMENT

An unnoticed earlier difference of math model efficiency calculated by Eq. (2) and measured efficiency $\eta = \ln\pi / \left(\frac{k}{k-1}\ln\frac{T_{o'}}{T_0}\right)$ influenced negatively on accuracy of calculations. The inaccuracy was eliminated.

The positive effect of innovations has demonstrated the identification process. The accuracy of design regime calculation for

38 model tests is inside 0,5% with one set of empirical coefficients for stages with very different design parameters. The same is accuracy in efficiency calculations of about two dozens of industrial compressors. Good performance prediction of model stages and calculation of plant test performances of different industrial compressors verified 6th version of the model too [16].

LOADING FACTOR PERFORMANCE MODELING

The experiments with all known model stages and compressors demonstrated that loading factor $\psi_T = c_{u2} / u_2$ is practically a linear function of the flow rate coefficient $\varphi_2 = c_{r2} / u_2$. This function is independent of compressibility criteria for a given impeller [16] – Fig.5.

There is well-known model: an impeller with infinite numbers of blades, non-viscid flow. The linear character of the function $\psi_{T\infty} = 1 - \varphi_2 \cdot ctg\beta_{bl2}$ is evident. The linear character of function $\psi_T = f(\varphi_2)$ shown at Fig. 4 is linear (inside test accuracy) for all tested impellers. It is not easy to explain this phenomenon meaning wake propagation at positive incidence angles (Fig. 1). This is not a reason not to use the phenomenon in modeling. Loading factor performance is defined by the equation:

$$\psi_T = \psi_{Tdes} + \frac{\psi_{T0} - \psi_{Tdes}}{\varphi_{2des}} \left(\varphi_{2des} - \varphi_2 \right) \tag{19}$$

Values of ψ_{T0} differ not too much for different impellers. There is an empirical equation for their calculations. In design method presented in [5] and in [3] the value of ψ_{Tdes} is a design parameter. The task of a designer is to find necessary number of blades and blade exit angle to obtain this value. The scheme is presented above in Fig. 3. Blade angle that corresponds to given ψ_{Tdes} is:

$$\beta_{bl2} = arctg \frac{\varphi_2'}{1 - \psi_{Tdes} + K_\mu \dfrac{\psi_{Tdes}}{z(1-\bar{D}_1)K_{pc}}} \tag{20}$$

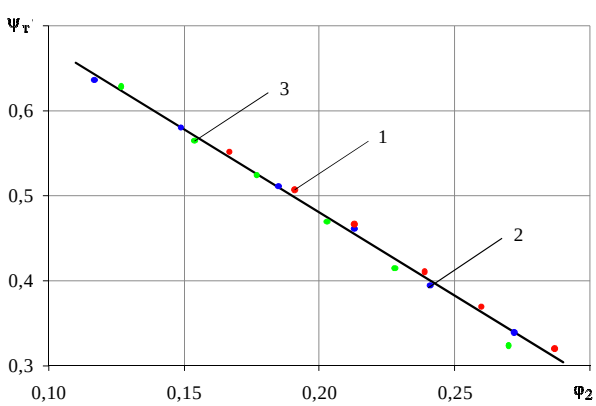

FIGURE 5. LOADING FACTOR VERSUS FLOW RATE COEFFICIENT AT THREE MACH NUMBERS.
$1 - M_u = 0{,}6$; $2 - M_u = 0{,}7$; $3 - M_u = 0{,}8$

The empirical coefficient $K_\mu > 1$ takes into account flow viscosity.

The alternative idea of modeling exploits linear character of the function $\psi_T = f(\varphi_2)$ too. The scheme is presented at Fig. 6.

Vectors $\vec{c}_2, \vec{w}_2$ are connected on the straight line inclined under the angle β_T. The tangent of this angle is:

$$tg\beta_T = \frac{\varphi_{2\max}}{\bar{u}_2 - \psi_{T0}} = \frac{tg\beta_{bl2}}{1 - \psi_{T0}} \tag{21}$$

The function $\psi_T = f(\varphi_2)$ is presented as:

$$\psi_T(\varphi_2) = \psi_{T0} - \frac{\varphi_2}{tg\beta_T} = \psi_{T0} - \varphi_2 \frac{1 - \psi_{T0}}{tg\beta_{bl2}} \tag{22}$$

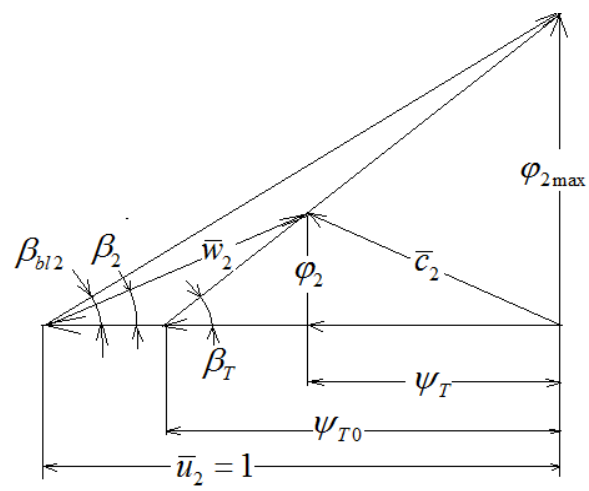

FIGURE 6. VELOCITY TRIANGLES AT AN IMPELLER EXIT

This scheme simplifies modeling process excluding some parameters that was necessary to take into account earlier.

NEW 5th AND 6th VERSIONS OF UNIVERSAL MODELING AND SAMPLES OF APPLICATION

The 4th version of the model and computer programs was widely applied in R&D practice since mid-1990th. Several dozens of designed compressors with power up to 25 MW were realized by some Russian and foreign manufacturers. Plant test performance of 16 most effective industrial compressors were compared with calculations by the programs of the 5th version [11, 12, 13]. Good correlation of design parameters was demonstrated. Satisfactory modeling of the whole performances was achieved by correction of empirical coefficients responsible for incidence losses. The sample is presented in Fig. 7.

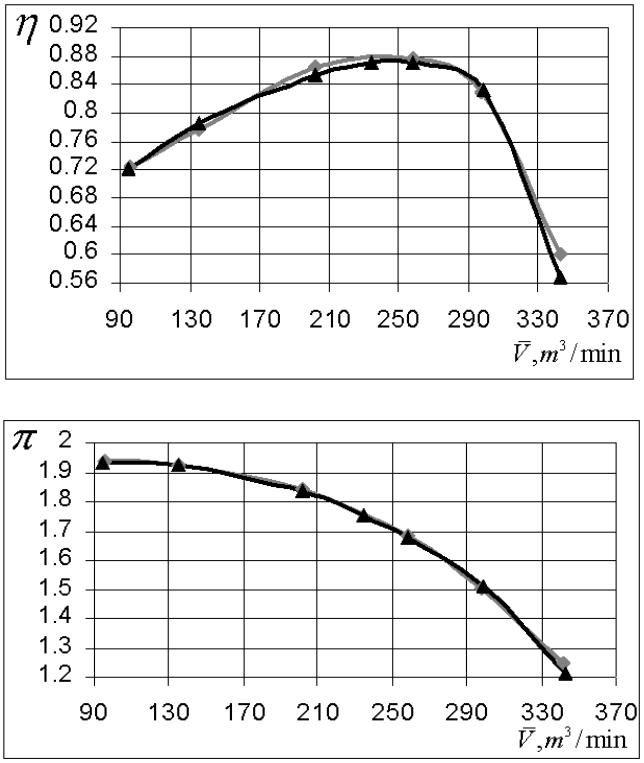

FIGURE 7. FOUR STAGE BOOSTER COMPRESSOR AIR TEST PERFORMANCES (GREY) AND MODELING RESULT (BLACK)

The four stage booster compressor was designed by the 4th version of Method. High efficiency was achieved due to a proper design and optimal design parameters Φ_{des}, ψ_{Tdes}. Performances of 68 stages of 16 compressors are added to database of model stages for use in current designs.

The one-stage 32 MW pipeline compressor was designed by 5th version program for one of industrial partners [17]. The tests of the model at the 1:2 scale validated project parameters – Fig. 8. Project performances, test results and CFX-calculations are related to the complete flow path. Its cross-section is shown in Fig. 8 above. CFX-calculation was made by the industrial partner [17].

Highest efficiency was achieved due to optimal design parameters Φ_{des}, ψ_{Tdes} as the partner has chosen high-RPM drive. Proposed by the partner single-stage scheme is the most effective due to axial inlet and zero hub ratio.

The prediction of the 5th version is quite good and the design principles in a whole demonstrated their effectiveness once more.

The 6th version input menu for stage parameters with 3D impeller and graphics with calculated stage performances at different velocity coefficient are presented in Fig. 9. The 6th version input menu for stage parameters with 2D impeller and graphics with calculated stage performances at different velocity coefficient are presented in Fig. 10.

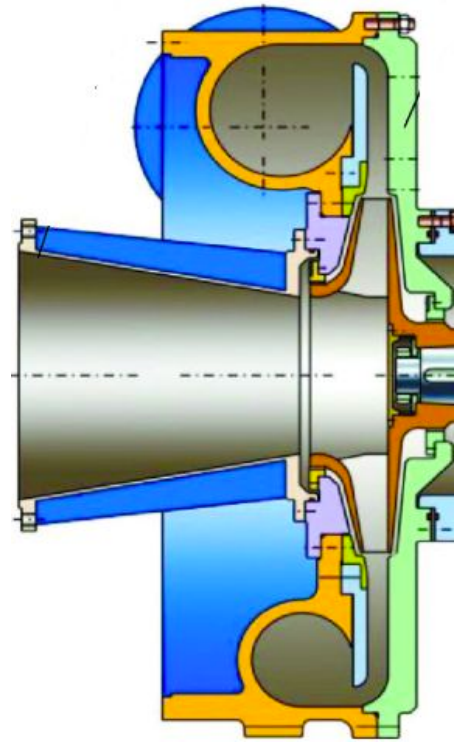

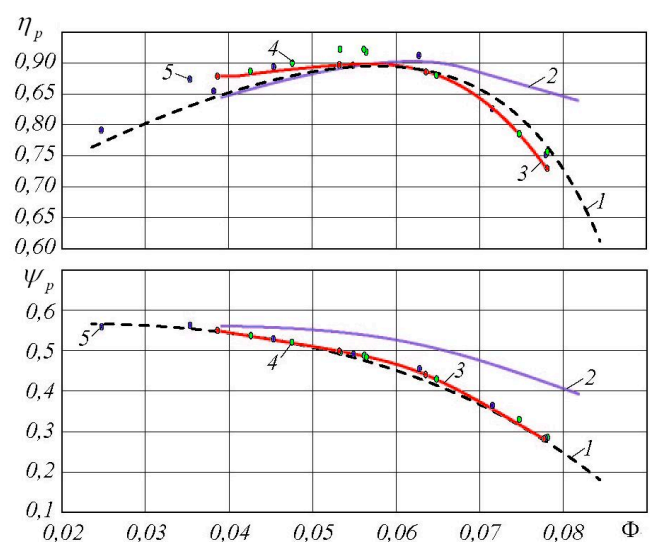

FIGURE 8. COMPRESSOR 32 MW MODEL CROSS SECTION (AHEAD) AND TEST RESULTS (BELOW). 1- DESIGN PERFORMANCE, 2- ANSYS CFX, 3- EXPERIMENT M_u = 0.705, 4 - EXPERIMENT M_u = 0.710, 5 - EXPERIMENT M_u = 0.700

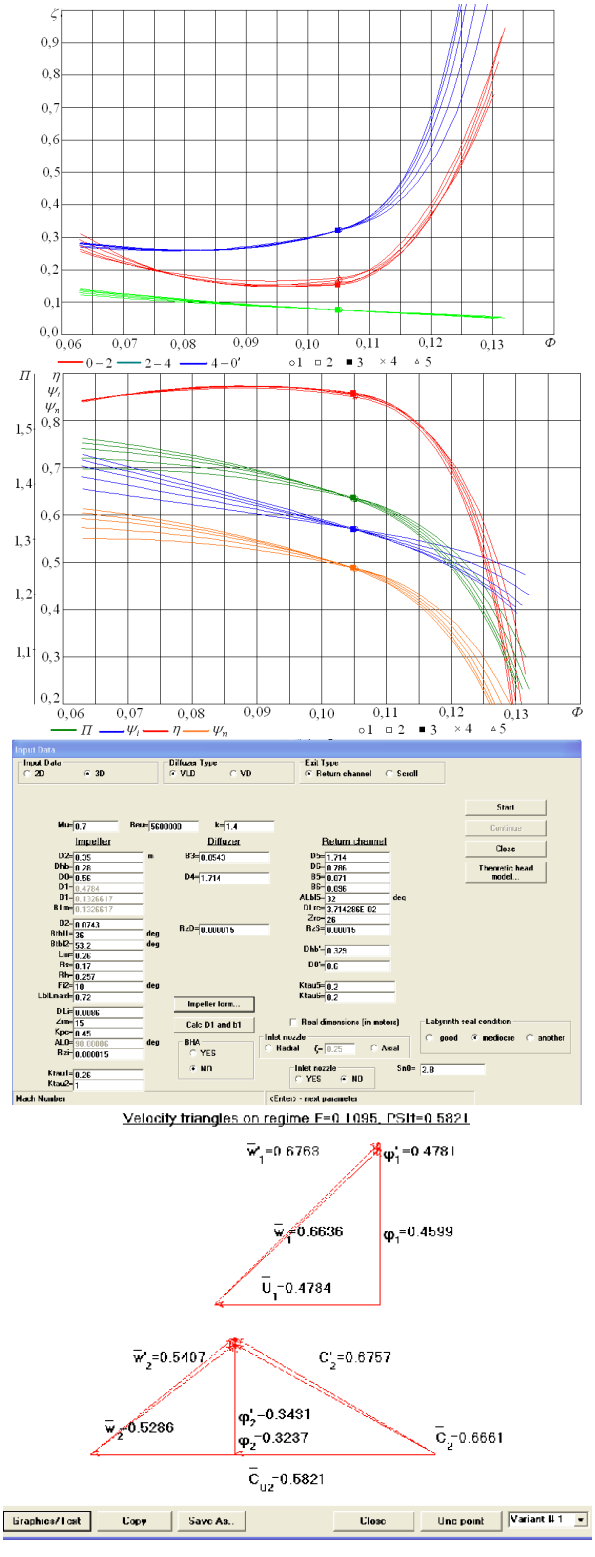

FIGURE 9. INPUT MENU FOR STAGE PARAMETERS WITH 3D IMPELLER AND A GRAPHIC WITH A STAGE PERFORMANCE AND VELOCITY TRIANGLES. COMPUTER PROGRAM CSPS-G6E

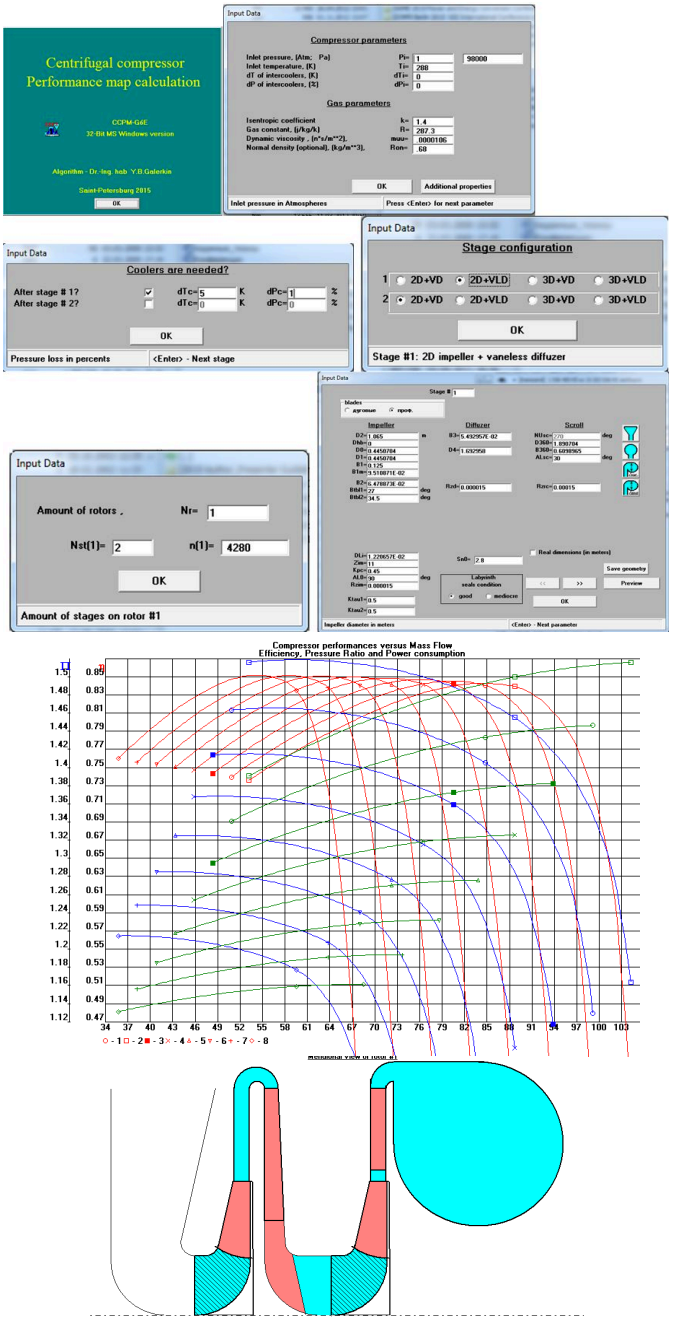

FIGURE 10. INPUT MENU FOR COMPRESSOR PARAMETERS AND A GRAPHIC WITH A STAGE PERFORMANCE AT DIFFERENT VELOCITY COEFFICIENT. COMPUTER PROGRAM CCPM-G6E

The program gives the possibility to optimize 11 main geometry parameters of a stage. For instance, the efficiency of the stage with Φ_{des} = 0,105 was increased on 0.97% by more than 80 stage variants comparison.

CONCLUSION

New versions of the Universal modeling method computer programs are applied in current design practice. The experience of application demonstrates their new abilities and points out on possibility of further progress. The actual problem is to increase CFD-calculation modeling abilities. The authors have good experience in CFD application for stages' stator elements. CFD impeller performance prediction is not completely reliable.

ACKNOWLEDGMENT

Work is performed with support of a Grant of the President of the Russian Federation for young PhD MK-7066.2015.8.

REFERENCES

[1] Japikse D. Design system development for turbomachinery (turbopump) designs - 1998 and a decade beyond. JANNAF Conference. Cleveland. – Ohio. – July 15 -17. – 1998.

[2] PCA Engineers Limited. [digital resource]. http://www.pcaeng.co.uk/software.

[3] Galerkin Y. Turbo compressors. LTD information and publishing center. - Moscow. – 2010 [Russian].

[4] Ris V. Centrifugal compressors. - Leningrad. – 1981. [Russian].

[5] Seleznev K., Galerkin Y. Centrifugal compressors. Leningrad. – 1982. – P. 271. [Russian].

[6] Kampsti N. Aerodynamic of compressors. – Moscow. – «Mir». – 2000. – P. 688. [Russian].

[7] Aungier R. Centrifugal compressors: a strategy for aerodynamics design and analysis. – 2000.

[8] Galerkin Y., Solovieva O. Improvement of vaneless diffusers calculation based on CFD experiments. Part 2. Compressors and pneumatics. - 2014. – № 4. – P. 15-21. [Russian].

[9] Galerkin Y., Marenina L. Investigation and perfection of centrifugal compressor stages by CFD methods. International Conference on Numerical Methods in Industrial Processes. World Academy of science, engineering and technology. Paris 2015 Conference. http://www.waset.org/Publications/?path=Publications. - Vol:9 No:01 2015. – №. 249.

[10] Lunev A. Structure of a method of design and test of flow part of superchargers for pumping of natural gas. Compressors and pneumatics. – 2001. – № 10. – P. 4-7.

[11] Soldatova K. Universal modeling method loss and work input models verification on results of industrial compressors test. Scientific and technical transactions of the TU SPb. 2010. – No. 4. – Page – 300-308.

[12] Galerkin Y., Soldatova K., Drozdov A. Specification of algorithm of calculation of parameters of a stream in the centrifugal compressor stage. Scientific and technical transactions of the TU SPb. – 2010. – No. 4. – Page – 150-157. [Russian].

[13] Galerkin Y., Soldatova K., Drozdov A. Turbo compressor efficiency application and calculation. Compressors & Pneumatics. – 2011. – No. 8. – Page 2-11. [Russian].

[14] Galerkin Y., Soldatova K. Analysis of gas flow calculations in a backlash between a covering disk and a case of centrifugal compressor stage. Chemical and oil and gas mechanical engineering. – No. 5. – 2007. – Page 27-29. [Russian].

[15] Lojtsanskij L. Mechanics of liquid and gas. – Moscow. – 1978 [Russian].

[16] Galerkin Y., Karpov A. Development of method for centrifugal compressor impeller pressure characteristic modeling on results of model stages tests. Compressors & Pneumatics. – 2011 – № 6. – P. 13-17. [Russian].

[17] Tirtishnij I., Parafejnik V., Nefedov A., Rjgalskij S., Kotenko N., Timoshadchenko D., Mixajlenko S. The thermodynamic analysis of efficiency of the centrifugal compressor as difficult system as a part of the gas-compressor unit (32). 16 International compressors conference. – Russia. – 2014. – Book 1. – P. 328-339.